Revista Brasileira de Cartografia
ISSN 1808-0936 | https://doi.org/10.14393/revbrascartogr
Sociedade Brasileira de Cartografia, Geodésia, Fotogrametria e Sensoriamento Remoto

Assessment of Water Spectral Indices Using a Landsat-9 scene: a Case Study in a Semi-arid Region

Avaliação de Índices Espectrais da Água Utilizando uma Cena Landsat-9: um Estudo de Caso em uma Região Semiárida

Juarez Antônio da Silva Júnior [1]

1 Universidade Federal de Pernambuco - UFPE, Recife-PE, Brasil. juarez.silvajunior@ufpe.br
ORCID: https://orcid.org/0000-0002-2898-0309

Recebido: 02.2024 | Aceito: 05.2024

Abstract: Spectral indices for detecting surface water bodies play a crucial role in environmental studies, on the other hand, these indices behave differently depending on the study site or the bands used. Therefore, this study proposed an evaluation of the performance of spectral indices in detecting surface water, using a scene from the Landsat-9 satellite and implementing a new index called NIR-Green Water Index (NGWI). After a visual inspection, positive performance was found in all indices in the detection of surface water, especially those formulated using the green band, such as the Normalized Difference Water Index (NDWI), (NGWI) and Water Ratio Index (WRI). During the Pearson correlation and Separability Index analysis between the "Water" and "Non-water" classes, the Automated Water Extraction Index (AWEI) demonstrated the highest average separability, reaching 1.24, and the lowest correlation, with 0.15, which places it as the index with the best detection estimates. The NGWI stood out especially when compared to other indices, showing a moderate behavior with an average separability of 1.15, surpassing the WRI (1.12) and the MNDWI (1.13), in addition to an average Pearson correlation of 0.17, just behind AWEI (0.16) and WRI (0.15). Although all the indices mentioned have demonstrated usefulness in water detection, it was observed that more complex indices, with a more elaborate formulation and less sensitivity to shadows, such as AWEI, produced results comparable to simpler indices, such as NDWI and MNDWI.
Keywords: Remote Sensing. Caatinga Biome. Water Reservoir.

Resumo: Os índices espectrais para detecção de corpos hídricos superficiais desempenham um papel crucial em estudos ambientais, por outro lado, esses índices se comportam de forma diferente dependendo do local de estudo ou das bandas utilizadas. Diante disso, este estudo propôs uma avaliação do desempenho de índices espectrais na detecção de águas superficiais, utilizando uma cena do satélite Landsat-9 e implementação de um novo índice chamado Índice NIR-Verde de Água (NGWI). Após uma inspeção visual, constatou-se um desempenho positivo em todos os índices na detecção de águas superficiais, especialmente aqueles formulados utilizando a faixa verde, como o Índice de Água por Diferença Normalizada (NDWI), (NGWI) e Índice de Proporção de Água (WRI). Durante a análise de correlação de Pearson e Índice de Separabilidade entre as classes "Água" e "Não água", o Índice Automatizado de Extração de Água (AWEI) demonstrou a maior separabilidade média, atingindo 1,24, e a menor correlação, com 0,15, o que o coloca como o índice com as melhores estimativas de detecção. O NGWI, destacou-se especialmente na comparação com outros índices, apresentando um comportamento moderado com uma separabilidade média de 1,15, superando o WRI (1,12) e o MNDWI (1,13), além de uma correlação de Pearson média de 0,17, ficando apenas atrás do AWEI (0,16) e do WRI (0,15).Embora todos os índices mencionados tenham demonstrado utilidade na detecção de água, observou-se que índices mais complexos, com formulação mais elaborada e com menor sensibilidade às sombras, como o AWEI, produziram resultados comparáveis a índices mais simples, como o NDWI e o MNDWI.
Palavras-chave: Sensoriamento Remoto. Bioma Caatinga. Reservatório de água.

1 INTRODUCTION

Surface water resources are of great value to humanity, as they offer a wide range of essential services, despite being the smallest portion of freshwater on the planet. These services include support for industrial and agricultural production, regional climate regulation and ecosystem maintenance. Furthermore, surface water

bodies play crucial roles in hydrological and biogeochemical cycles at local, regional and global levels. These areas are highly sensitive to both climate change and human activities, therefore serving as fundamental indicators of the various influences of environmental change and human action (MUSIE; GONFA, 2023). Traditional surface water monitoring methods are mainly based on manual surveys on the ground or at established measuring stations. Although the accuracy of the acquired data is high, it is time-consuming and costly work. Furthermore, many water bodies are in remote and rugged locations, and only data from limited points in incomplete time series can be obtained due to the limitations of economic and terrain factors (SABALE; VENKATESH; JOSE, 2022).

Lately, advances in Remote Sensing have offered an approach for monitoring of widely distributed water bodies over large areas prolonged periods. In this scenario, remote sensing provides observational data that widely covers space and is frequent over time, referring to the Earth's surface. This information can be used to map and monitor surface water dynamics (ALBERTINI et al. 2022). The widespread use of multispectral satellite imagery is seen in mapping and detection of water bodies, providing crucial data on the extent and quantity of surface aquatic resources. This information plays a significant role in analyzing water quality, calibrating and validating hydrological and hydrodynamic models, as well as creating risk maps for prevention, planning and environmental monitoring activities. Since it was launched in 1972, the freely available Landsat has gradually become one of the most popular remote sensing sources for surface water detection (SAGAN et al. 2020). The optical sensor onboard Landsat has a typical spatial resolution of 30 m for mapping water, among many other freely available but coarser sensors, e.g. Moderate-Resolution Imaging Spectroradiometer (MODIS) (250–1000 m), Advanced Very High Resolution Radiometer (AVHRR) (1100 m), Envisat MEdium Resolution Imaging Spectrometer (MERIS) (300 m) although high-resolution sensors, such as WorldView (0.31–2.4 m), have been used for water detection purposes, the difficulty in accessing this data hinders widespread applications when compared to Landsat (WANG et al. 2018).

In general, images from orbital sensors provide a multi-temporal view of large areas of the Earth's surface. The quantitative and qualitative assessment of terrestrial features using orbital images has been carried out, among other ways, using spectral indices. The spectral indices are radiometric values calculated through operations involving different bands of orbital images and Unmanned Aerial Vehicle (UAV) images, and their applications provide parameters capable of investigating spectral properties, identifying certain types of information composed of different materials, such as water, buildings, or vegetation. The spectral indices are ratios involving reflectance values of the visible and infrared spectral regions, as these are sensitive to factors of physical structure, leaf area, surface water, soil moisture and photosynthetically active biomass. Different spectral indices have been developed, applied and analyzed with the aim of further exploring the spectral properties of water. Among the most used spectral water indices, the following stand out: Normalized Difference Water Index (NDWI), Modified Normalized Difference Water Index (MNDWI), Automated Water Extraction Index (AWEI) and Water Raio Index (WRI).

The NDWI has two formulations, proposed by McFeeters (1996) and Gao (1996). McFeeters' NDWI (1996) is a ratio involving the green and near-infrared bands, used to highlight water bodies and minimize the response of other targets. The NDWI proposed by Gao (1996) is used to estimate the moisture content of vegetation, and is calculated from the ratio between the near-infrared and shortwave infrared bands. The MNDWI was developed by Xu (2006). This index uses the shortwave infrared band instead of the near-infrared band. In addition to detecting surface water, this index removes noise created by vegetation and built areas. In some cases, elements with low reflective characteristics, such as shadows, burnt areas and dark roofs in urban areas, are mistakenly classified as water (Feyisa et al. 2014). Therefore, Feyisa et al. (2014) developed AWEI, which effectively removes dark areas of accumulation and other non-water pixels. While Shen and Li (2010) developed WRI for water body extraction from Landsat ETM+ images. This index is based on the ratio between the total spectral reflectance of two visible bands (i.e., green and red) and the total spectral reflectance of the near-infrared and shortwave infrared bands.

Despite the already established performance of spectral index, comparative studies persist that seek to evaluate the effectiveness of these different spectral indices. To date, no index has proven effective in all scenarios, with performance variations influenced by scene, sensor and weather conditions. This diversity of results makes room for the proposition of new modified spectral indices, aiming to optimize performance in

specific scenarios (LI et al. 2021). Bijeesh and Narasimhamurthy (2020) reported that the critical step in applying water spectral indices for water detection is to identify the most differentiating bands within the multiband image. Sufficient research is needed before it can be proven that the chosen bands are the most suitable for detecting water masses. Most proposed spectral indices are developed for specific sensor data and with the advent of newer satellites and sensors, newer spectral indices will have to be developed to incorporate improvements in data acquisition. Thus, methods based on spectral indices are of interest to researchers not only because they are easy to use and provide better results, but also because there is still room to improve existing spectral indices and propose new and better spectral indices (YANG; DU, 2017).

Recent advances in remote sensing technology have provided new approaches for studying the dynamics of surface waters and their margins, encompassing various aspects such as mapping rivers and water bodies, detecting wetlands and flooded areas, and monitoring water quality. The implementation of new water spectral indices is closely linked to the development of new sensors with specific bands. For example, the NGWI, pioneered in this article, is derived from images from the newly launched Landsat-9. Additionally, the Multispectral Water Index (MuWI) is calculated using specific bands from the MultiSpectral Instrument (MSI) sensor on the Sentinel-2 satellite as described in Wang et al. (2018), and normalized water quality indices are obtained from the bands of the Ocean and Land Colour Instrument (OLCI) sensor on the Sentinel-3 satellite (RAWAT et al. 2023).Therefore, this study aimed to propose a new water index for images from the Landsat-9 (OLI-2) satellite as well as analyze spectral characteristics of the NDWI, MNDWI, AWEI, WRI and NGWI for detecting surface water in the semi-arid scenario. The checks were compared under different types of land cover based on visual analysis, variation of medians by boxplot graphs, statistical separability and linear regression analysis.

2 MATERIAL AND METHODS

2.1 Study area

The Landsat path/row grid area (216/066) of size 185 km x 180 km was considered in this study and is located in northeastern Brazil where it has a high distribution of water bodies of different spatial configurations, partially covering the states of Pernambuco, Ceará, Alagoas, Sergipe and Bahia, entirely inserted in the semi-arid region (Figure 1). This region belongs to the northeastern semi-arid region of deciduous vegetation, characterized by low rainfall, low air humidity and high temperatures. Furthermore, the area has a distribution of water dams, including the Serrinha II Dam, the Barra do Juá Dam and the Itaparica Reservoir, some of which are supplied by the transposition of the São Francisco River.

Figure 1 – The study area covers water bodies with different surface sizes and local landscapes, mainly characterized by a wide presence of artificial reservoirs distributed throughout the scene.

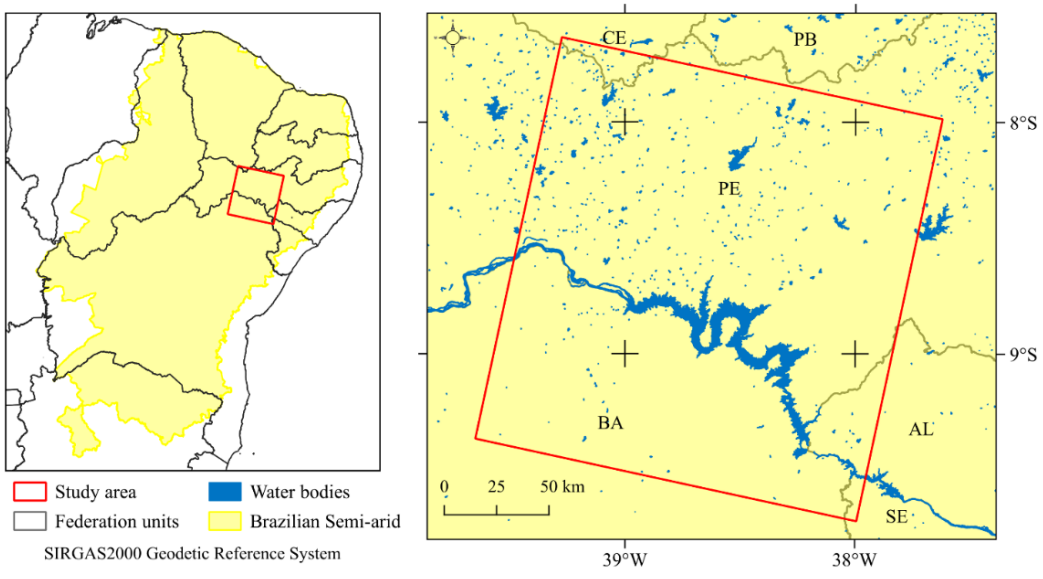

Source: Author (2024).

2.2 Landsat-9

Landsat 9 is an earth observation satellite in a joint mission of the US National Aeronautics and Space Administration (NASA) and the US Geological Survey (USGS), launched on September 27, 2021, from Vandenberg Space Force Base, in California. Landsat-9 includes two instruments: The Operational Land Imager 2 (OLI-2) to capture reflective bands and the Thermal Infrared Sensor 2 (TIRS-2) to obtain thermal infrared data. Table 1 describes the technical specifications of the Landsat-9 satellite. The TIRS2 sensor bands as well as the Panchromatic band and the Cirrus band were not used in our study.

Table 1 – Technical specifications of OLI-2 and TIRS-2 images from Landsat-9

Sensor	Band	Name	Spectral resolution (μm)	Spatial Resolution (m)
OLI-2	band 1	Coastal Aerosol	0.43 - 0.45	30
	band 2	Blue	0.450 - 0.51	30
	band 3	Green	0.53 - 0.59	30
	band 4	Red	0.64 - 0.67	30
	band 5	Near-Infrared	0.85 - 0.88	30
	band 6	SWIR 1	1.57 - 1.65	30
	band 7	SWIR 2	2.11 - 2.29	30
	band 8	Panchromatic	0.50 - 0.68	15
	band 9	Cirrus	1.36 - 1.38	30
TIRS-2	Band 10	TIRS 1	10.6 - 11.19	100
	Band 11	TIRS 2	11.5 - 12.51	100

Source: USGS (2023).

In this study, we used a Landstat-9 scene with ID LC92160662023275LGN00 captured on October 2, 2023 without the presence of clouds, made available by the Earth Explorer platform. Landsat-9 collection 2 level 2 images are distributed with surface reflectance using the Land Surface Reflectance Code (LaSRC) (version 1.5.0), which makes use of the coastal aerosol band to perform aerosol inversion tests, uses weather data MODIS auxiliaries and a unique radiative transfer model (Vermote et al. 2016). The Land Surface Reflectance Code (LaSRC) Product Guide contains details about the LaSRC algorithm and the Surface Reflectance data products created from it available at USGS (2023).

2.3 Water Spectral Indices

Table 2 presents four widely used water spectral indices in the literature: NDWI, MNDWI, AWEI, and WRI. In addition to the indices in Table 2, this study proposes a new water spectral index called NGWI, which will also be used in the performance analysis of the indices.

Table 2 – Formula of the water index used in this study. ρ_{Green} = green band; ρ_{NIR} = Near-InfraRed band; ρ_{SWIR1} = ShortWave InfraRed 1 band; ρ_{SWIR2} = ShortWave InfraRed 2 band.

Spectral Water index	Formula	Reference
Normalized Difference Water Index (NDWI)	$\frac{(\rho_{Green}-\rho_{NIR})}{(\rho_{Green}+\rho_{NIR})}$	McFeeters (1996)
Modified Normalized Difference Water Index (MNDWI)	$\frac{(\rho_{Green}-\rho_{SWIR1})}{(\rho_{Green}+\rho_{SWIR1})}$	Xu (2006)
Automated Water Extraction Index (AWEI)	$(\rho_{Blue}+2.5\times\rho_{Green}-1.5\times(\rho_{NIR}+\rho_{SWIR1})-0.25\times\rho_{SWIR2})$	Feyisa et al. (2014)
Water Ratio Index (WRI)	$\frac{(\rho_{Green}+\rho_{Red})}{(\rho_{NIR}+\rho_{SWIR1})}$	(Shen and Li, 2010)

Source: Author (2024).

The choice of bands to define the new spectral index, the NGWI, was derived from the extensive existing literature on the spectral sensitivity of the green and near-infrared bands in water bodies, together with a critical analysis of the reflectance properties of various types of land cover. This approach was guided by the theory that water absorbs almost all incident radiant flux, while the Earth's surface reflects significant amounts

of energy in the near-infrared and shortwave infrared bands, with the reflectance in the green band being much greater for water. than for the Earth's surface (MCFEETERS, 1996; LEE et al. 2007; BARBOSA; NOVO; MARTINS, 2019).

The main objective in formulating the NGWI was to maximize the separability between water and non-water pixels through the arithmetic manipulation of the green and near-infrared bands, along with the application of different coefficients. The development of NGWI was largely based on determining the point of convergence, which characterizes the radiative properties of the feature to be highlighted, in this case, water, in the green and near infrared bands (MARTÍN, GÓMEZ and CHUVIECO, 2006; MCFEETERS, 1996; ARST, 2003; XU, 2006). The definition of the convergence point was based on the analysis of dark areas in satellite images (low albedo), identified in studies by Feyisa et al. (2014), Mostafa (2017), Mcfeeters (1996), Zhou et al. (2017), Chuvieco, Martín and Palacios (2002), Ouma and Tateishi (2006) and Martín, Gómez and Chuvieco (2006), together with empirical results derived from reflectance patterns observed in pixel datasets representative of different types of land cover. The index was calculated through the inverse of the Euclidean distance between the spectral values at that point of convergence as detailed in Eq. (1).

$$NGWI = \frac{1}{(0{,}05 - \rho_{NIR})^2 + (0{,}3 - \rho_{Green})^2} \quad (1)$$

Based on the analysis performed, the convergence thresholds were established at 0.05 (NIR) and 0.3 (Green). In Eq. (1), when calculating the sum of the second-order polynomial derived from the difference between the green and infrared bands using these convergence thresholds, the resulting values are considerably high for most non-aquatic pixels, while they are lower for the of water. To better distinguish water from other surfaces with similar spectral patterns and visually highlight water pixels, the inverse of the expression is calculated. Therefore, non-aquatic pixels tend to have values close to zero, while water pixels have slightly higher values. Applying a scaling factor of 10^9, the NGWI ranges from 0 to 1, with values above 0.5 being detected as “Water” and values below 0.5 being detected as no water.

2.4 Visual and statistical analysis

The spatial distributions of water indices was visually compared with a colored composition of the Landsat-9 scene, as well as Lidar images from the Pernambuco Digital Program (PE3D) and Google Earth in order to interpret the characteristics and patterns, in addition to understanding and analyzing spatial phenomena based on images of water indices. To carry out statistical analyzes based on sample selection, 500 points were selected in vector format (shapefile) to assess accuracy through a stratified random sampling method, with 100 points for each class of land use and occupation present in the area. of study, being: Tree Vegetation, Shrub Vegetation, Pasture, Unvegetated Area and Water. The identification of these classes was based on overlapping with Mapbiomas maps. Therefore, these points were used to extract the values per pixel for each water spectral index analyzed in this study (BROWN et al. 2022).

Based on the water index values obtained by the samples, a median analysis was performed using a boxplot graph and linear regression analysis between the “Water” and “Non-Water” classes represented by the different classes of land use and land cover (LULC). The analyzes made it possible to statistically understand the behavior of water indices and their power to detect surface water in satellite images.The M statistic was used to measure the spectral separability between the “Water” classes and the LULC classes based on the training samples, through Eq. (2). The M statistic quantifies the spectral distance between two distributions, the distance between the class means represents the signal intensity and the sum of the standard deviations represents the noise (KAUFMAN; REMER, 1994).

$$M_b = \frac{|\mu b - \mu ub|}{\sigma b + \sigma ub} \quad (2)$$

Where μb and μub are the pixel average values of the spectral difference for the water and non-water

subsamples; and σ b and σ ub the corresponding standard deviations. The range of values generated by this method is 0.0 to 2.0, where a value of 0.0 means that the class pair has perfect similarity and a value of 2.0 or greater indicates that the class pairs are completely different.

2.5 Otsu threshold

Identification of water bodies based on spectral indices involves defining a threshold to distinguish between land and water areas in the image. However, finding this threshold is challenging, as it can vary due to several factors, such as land cover (CORDEIRO et al. 2021; TANG et al. 2022). In this study, we used an automated thresholding method based on Otsu's method to classify pixels as "Water" or "No Water" (OTSU, 1979). The Otsu method is widely used in binary applications in satellite images, as it seeks to minimize the variance within each class in bimodal histograms of grayscale images. Previous studies have demonstrated that Otsu's algorithm is effective in separating water bodies in Landsat images (XIE et al. 2016). The final maps of water bodies were generated using the SciKit Image library, developed in Python 3.7 (WALT et al. 2014). This approach provides an efficient and reliable way to extract water bodies from spectral images, contributing to diverse applications in remote sensing and environmental analysis.

3 RESULTS

Figure 2 and 3 shows a visual comparison of four stretches present in the study area represented by the composition of false-color images R(green)-G(red)-B(NIR) in relation to the spatial distribution of the AWEI water spectral indices, NGWI, NDWI, MNDWI and WRI.

Figure 2 – Visual comparison between water indices in four locations in the study area being a) – f) Serrinha II Dam, Pernambuco (Lat/Long), Urban area between water dams in the municipality of Serra Talhada, Permanbuco (Lat/Long), Section of the Itaparica Reservoir (Pernambuco/Bahia).

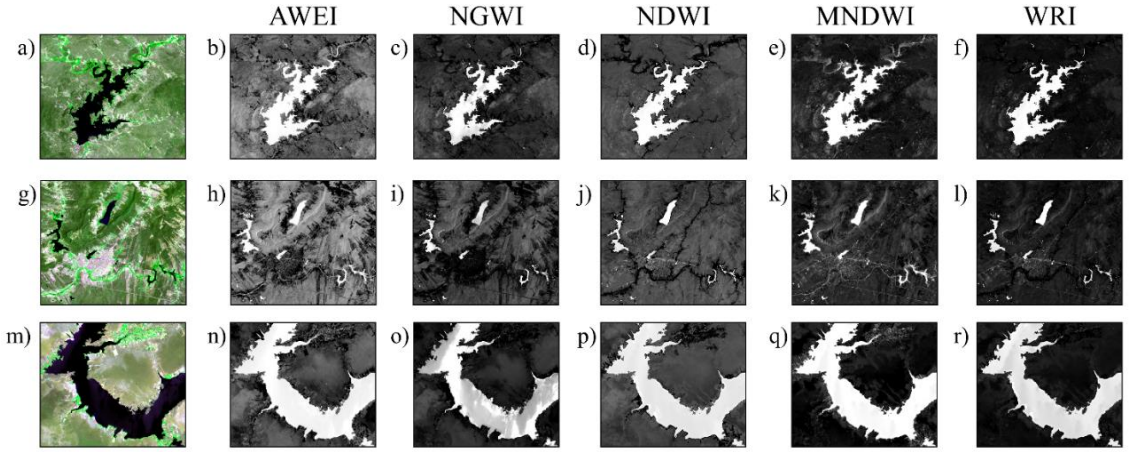

Source: Author (2024).

Figure 3 – Visual comparison between water indices in four locations in the study area being a) – f) Serrinha II Dam, Pernambuco (Lat/Long), Urban area between water dams in the municipality of Serra Talhada, Permanbuco (Lat/Long),

 DOI: http://dx.doi.org/10.14393/rbcv76n0a-72559

Section of the Itaparica Reservoir (Pernambuco/Bahia).

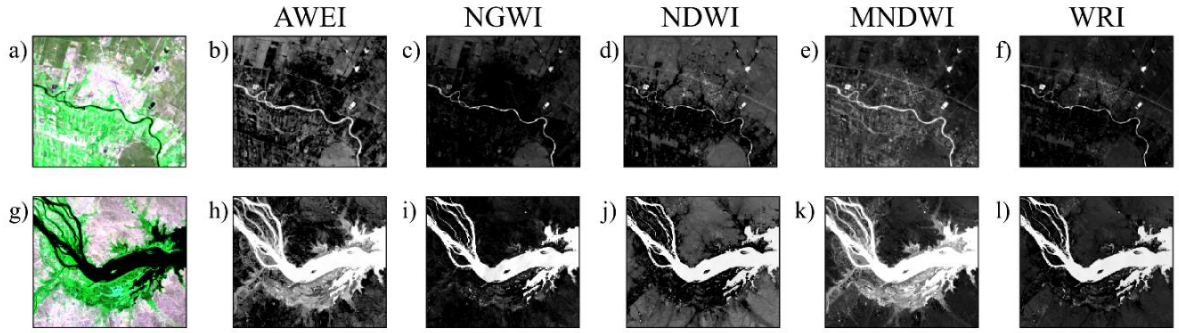

Source: Author (2024).

In Figure 2 a) – f) and m) – r), it is highlighted that all indices showed a clear separation from the water body, evidenced by whitish pixels. This suggests that all of these indices have the potential to provide relevant spatial data for surface water detection. In Figure 2g) - 2l), overall, the visual analysis revealed a positive performance of all indices in identifying smaller-scale water features, in addition to an apparent distinction in relation to urban areas in the area. However, the NGWI and WRI indices stood out by presenting a more pronounced contrast between the characteristics of water bodies and surfaces without water. In Figure 2 m) – r), despite the positive detection mentioned above, it is noticeable that there are visual variations, with emphasis on Figures 2 o) (NGWI) and 2 r) (WRI). These variations may be related to the sensitivity of these indices to the presence of chlorophyll and suspended solids in the water.

In Figure 3 a) – f), it is noted that the indices were effective in demarcating the river transposition line, even in a region with varied uses (agriculture in the southern sector and urban area in the northern sector). Both AWEI and MNDWI presented a delimitation with greater spacing, probably due to the sensitivity of these indices, where the pixels experienced a spectral mixture in the transition between the water and the land portion. While in Figure 3 g) – l), a region of the water body surrounded by humid areas, especially riparian forests, can be seen. The AWEI (Figure 3h) and MNDWI (Figure 3k) indices highlighted water pixels in these areas, indicating a limitation in the detection of water bodies in places with a notable presence of riparian forests.

To spatially examine the extraction of the water body separated by “Water” and “Non-water” classes obtained by the Otsu method, Figure 4 presents the visual comparison based on the different spectral indices at four example points in the OLI-2 scene. In the analysis of the images in row 4b)-4f), it is evident that all indices were able to identify the water body of the Serrinha II Dam - Pernambuco without major interference, demonstrating effectiveness in detecting compact and isolated water masses. However, in row 4h) - 4l), overestimations related to urban spot pixels were observed, with emphasis on the NDWI, MNDWI and WRI indices.

Figure 4 – Results of extracting information about terrestrial surface water in the OLI-2 scene for different water spectral index.

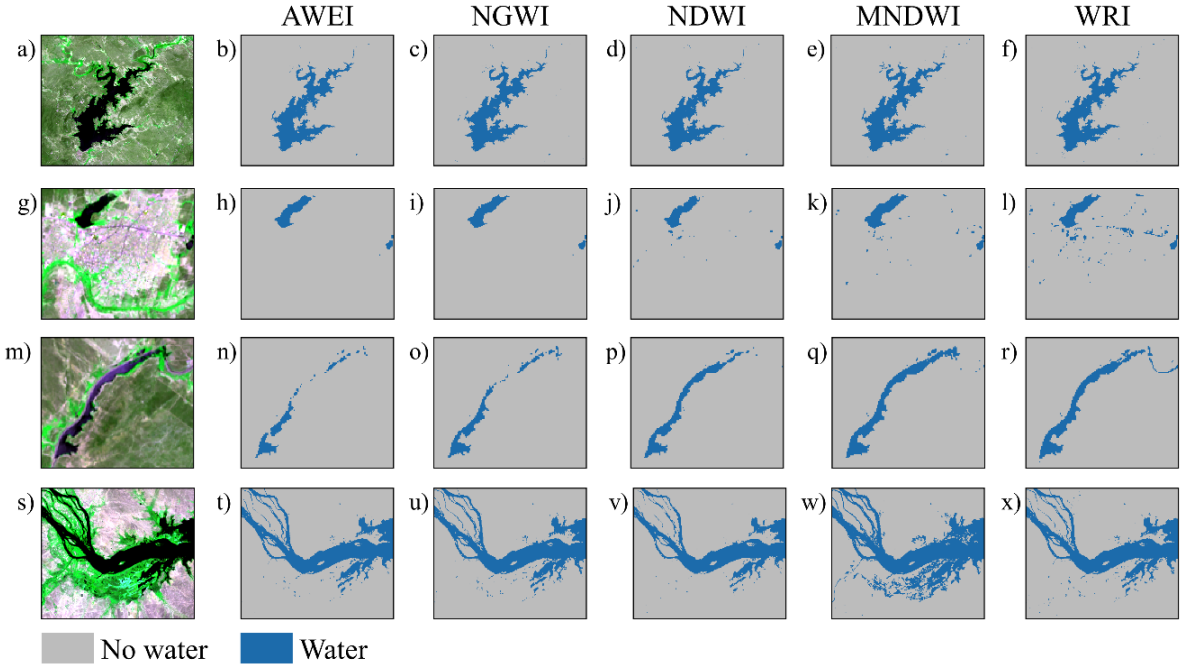

Source: Author (2024).

Chen et al. (2020), using the Otsu and K-means method to detect water in urban areas, also found limitations in NDWI and MNDWI, especially when applied to high spatial resolution images. Purnam, Prasad and Ganasala (2024) and Chen et al. (2020) highlighted that automatic thresholding methods, such as the Otsu method and the K-means algorithm, only perform well if the histogram has a bimodal distribution, in which it has a deep and accentuated valley between the two peaks that represent objects and background, respectively. However, if the spatial content of the background image has several different spectral elements, the histogram will no longer exhibit bimodality and then the threshold value determined by the Otsu method will be incorrect.

Visually, NDWI, MNDWI and, especially, WRI presented a satisfactory extraction when compared to the RGB composition in Figures 4p), 4q) and 4r). The color of the water of the Cacimba Nova Dam, in Pernambuco, may be related to underestimations observed in the AWEI and NGWI indices applied in the Otsu method, showing a high sensitivity to spectral variations of the water for these indices. The humid areas and the São Francisco Delta, also in Pernambuco, demonstrated the potential and limitations of water extraction rates. All indices presented isolated pixels distributed in the humid environment in the southern sector of the river, however MNDWI showed a high frequency of these pixels, indicating a significant limitation in this type of target. Still in the Delta formation, only NDWI did not detect some narrower features, while MNDWI stood out visually with a more consistent detection. The AWEI, NGWI and WRI indices showed good detection, with similar results.

Ma et al. (2019) highlighted that in humid areas and narrow rivers, the sensitivities of different indices to the proportions of water and land are different. This difference means that the threshold is indeed sensitive to the mixing characteristics of the land surface and indicates the need for the dynamic threshold method, which has also been suggested by other studies. The stability of thresholds is especially important when carrying out water mapping over large areas because complex land cover configurations are more likely to exist (ELSAYED et al. 2019). These statements will be applicable for wetland detection, as the land surface of wetlands typically transitions from pure water to a mixture of water and plants, and then to full vegetation cover. Thus, the transition from the dominant signal in water to the dominant signal in plants can be an important feature for wetland mapping. In order to understand the spectral behavior of each index, Figure 5 shows boxplots with the distribution of pixel values based on the land cover classes present in the study area.

Figure 5 – Boxplot graph of water spectral indices values in relation to LULC classes.

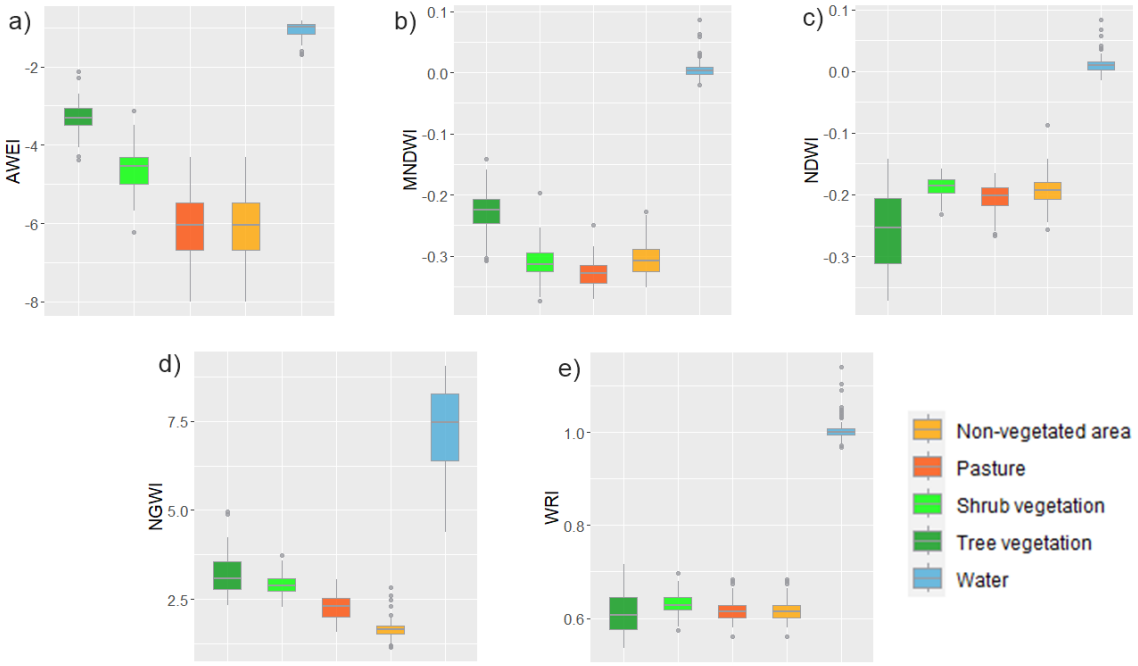

Source: Author (2024).

In general terms, it is clear that all spectral indices exhibited significant variation between the different land cover classes and the "Water" class. Furthermore, they all demonstrated stability in the pixel values assigned to the water class, maintaining an interquartile range below 0.27, except in the case of the NGWI index. The AWEI revealed variations in the median greater than 5 for the pasture and non-vegetated area classes. On the other hand, for vegetation classes, variations were concentrated below 3.5, indicating that this index has a lower water detection capacity compared to classes without vegetation. In contrast, the MNDWI demonstrated stability in median variations.

The classes of shrub vegetation, pasture and non-vegetated area remained at around 3, while tree vegetation exhibited a variation of 2.27. The NDWI exhibited a notable proximity between the medians in relation to the "Water" class, all concentrated below 2.6, with emphasis on the shrub vegetation class, which registered 1.95. The NGWI stood out for its best performance, presenting a median disparity above 4 for all classes, especially for pasture (5.17) and non-vegetated area (5.81). However, as mentioned previously, the "Water" class demonstrated high instability in pixel values, presenting the largest interquartile range in the analysis (1.9) and the largest standard deviation (1.16). The WRI showed the greatest stability in the median difference, all concentrated between 3.5 and 4 for all classes. These values are in accordance with the separabilities found in Table 3, which shows the values of the M index between the land cover classes and the “Water” class, showing the detection power of each spectral index in detecting water bodies in relation to other components.

Table 3 – Separability Index (M) between soil cover classes and the “Water” class.

LULC/ Indices	WRI	AWEI	MNDWI	NDWI	NGWI
Water/Tree vegetation	1,19	1,24	1,23	1,38	1,22
Water/Shrub Vegetation	1,09	1,25	1,10	1,13	1,13
Water/Pasture	1,10	1,21	1,11	1,17	1,11
Water/Non vegetated area	1,10	1,27	1,06	1,18	1,14

Source: Author (2024).

It was observed that all classes presented high separability indices (M > 1), with small variations both between categories and indices. Despite this, the tree vegetation class exhibited the highest mean separability, reaching 1.25, while the other classes varied between 1.14 and 1.15. The lowest separability was observed in the WRI index for shrub vegetation, reaching 1.09, while the AWEI index revealed the highest mean separability (1.24), followed by the NDWI (1.22). The latter stood out in the tree vegetation category, presenting the highest separability of the set (1.38). The WRI, NDWI and NGWI indices demonstrated

consistent values between the classes, with a slight advantage for the NGWI, which presented an average separability of 1.15, while the WRI was 1.12 and the NDWI was 1.13.

To analyze the strength of correlation between the (LULC) classes and the Water class for each index, a linear regression model was applied as well as the Correlation estimates (r) shown in Figure 6 and Table 4.

Figure 6 – Scatterplot graph of linear regression grouped between land use and land cover classes and the Water class for each water spectral index under analysis.

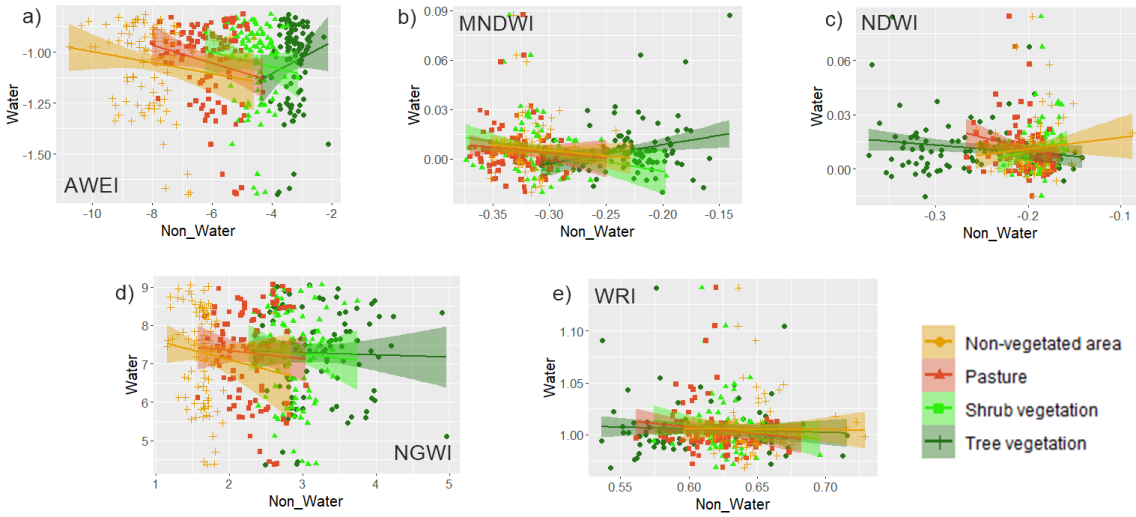

Source: Author (2024).

Table 4 – Correlation values (r) between the LULC and the “Water” class.

LULC/ Indeces	AWEI	MNDWI	NDWI	NGWI	WRI
Water/Tree vegetation	0,4	0,5	0,03	0,21	0,17
Water/Shrub Vegetation	0,12	0,01	0,38	0,19	0,1
Water/Pasture	0,03	0,13	0,03	0,17	0,09
Water/Non vegetated area	0,08	0,12	0,36	0,1	0,22

Source: Author (2024).

Overall, the estimates of (r) did not reveal a significant pattern regarding the ability of the indices to separate the "Water" class, as summarized in Table 3, which compiles the correlation values. The MNDWI and NDWI indices showed the highest average correlations in the set, driven by the value of (r) in the tree vegetation class (r = 0.5) in the MNDWI and by the values of (r > 0.35) for the tree vegetation classes shrub vegetation and non-vegetated area in the NDWI, as indicated in Table 3. However, in this analysis, these indices revealed less effectiveness in detecting water bodies due to the significant correlation values between them. On the other hand, the WRI index stood out for its greater dispersion, indicating a greater water detection capacity, while the AWEI and NGWI indexes demonstrated values of (r) close to each other.

4 DISCUSSIONS AND CONCLUSIONS

In this study, the pioneeringly tested NGWI index, in addition to the other indices, aimed to extract the water surface and quantify the detection power through a scene from the recent Landsat-9. Comparing the trends in the area in this article with the results of other researchers, it appears that the results obtained have a high consistency standard. In particular, Bhaga et al. (2020) reported that advances in indices, techniques and availability of multitemporal and multispectral images have led to improved monitoring and detection of droughts and surface water resources, however, there is still a need to improve indices to remedy cloud contamination and the problem of shadows in mountainous and urbanized areas. Although previous research has devised several methods for identifying and mapping water bodies, this issue remains challenging as no method is universally applicable in all contexts and datasets. The proposal of improved spectral indices may be promising perspectives to address this complexity in specific applications (BIJEESH; NARASIMHAMURTHY, 2020). Previous studies, exemplified by Feyisa et al. (2014), Deoli et al. (2021), Khan (2022) and others that will be discussed later, summarize the dynamics of accuracy in water detection

based on spectral indices, highlighting the limitations and potentialities. These studies offer a comparative analysis with the results achieved in the present research, especially in varied contexts of land use and extraction methods.

AWEI was designed to detect water bodies and avoid overestimation errors in shadows and other dark surfaces (FEYISA et al. 2014). Thus, as an initial study, the northeastern semi-arid region was selected as a simple and ideal case region, without a complexity of land covers covered by pure and open surface water bodies. There was no shadow area due to the mostly depressionless terrain, nor high albedo surfaces, such as snow and ice, due to the hot semi-arid climate. Furthermore, there were very limited urban areas in the area (ZHOU et al. 2017). Therefore, it was observed in this study that the AWEI index achieved a good performance in detecting water bodies, especially compared to the "Non-vegetated area" class, despite a visual limitation found in wetlands that was also seen for the MNDWI. In contrast, in research carried out by Rad, Kreitler and Sadegh (2021), AWEI demonstrated to be effective in delimiting water bodies in urban areas, making use of a series of Landsat images. In another study, AWEI demonstrated moderate performance, as evidenced by Yue et al. (2020), where the authors observed that due to the adopted threshold method, AWEI faced difficulties in accurately distinguishing between the water body and the mountain shadow in the Ordos basin, China. Furthermore, in studies conducted by Tew et al. (2022), AWEI fell short of MNDWI in identifying tropical aquaculture ponds in southwest Malaysia.

NDWI is an index often used to enhance water characteristics in satellite images, eliminating the effects of soil and vegetation. Several studies demonstrate the effectiveness of NDWI in various regions of the world, applying it to monitor ecosystem variables and hydrological conditions. It particularly stands out in extracting and mapping the boundaries of aquatic areas, as well as estimating water volume (TENG et al. 2021; MCFEETERS, 1996). In the present study, the NDWI proved to be appropriate, presenting results similar to other indices, especially the MNDWI. However, the latter stood out in comparisons of water detection in relation to vegetation classes, which may be related to the MNDWI values in the water body being lower than the NDWI values, further enhancing the separabilities in relation to the other classes, since the Bottom of Atmosphere (BoA) reflectance values in the SWIR band are greater than those in the NIR (CHOUDHARY; GHOSH, 2022). In analyzes carried out by Wicaksono and Wicaksono (2019), it was found that NDWI had an advantage in detecting water bodies in unbuilt areas, but demonstrated a weakness when identifying water bodies in built urban environments (XU, 2006). On the other hand, Khan (2022) observed more promising results for MNDWI, highlighting its ability to extract water elements mixed with vegetation in satellite images, compared to NDWI. This effectiveness of MNDWI also extends to surface water quality analyses, as evidenced by Soltanian (2019). In a comparative study conducted by Blackmore et al. (2016) using Landsat-8 images in both dry and humid areas, with vegetation cover, it was found that the NDWI was more capable of predicting variations in dry conditions, especially in periods of recent significant rainfall. This capacity was attributed to the response of NDWI to vegetation moisture rather than surface moisture. Por sua vez, os resultados de Ali et al. (2019) indicaram que o MNDWI pode aprimorar a identificação de corpos d'água e suprimir eficientemente características acumuladas em comparação com o NDWI.

The NGWI water spectral index developed in this study uses the green and NIR bands of the OLI-2 sensor to increase the accuracy of water extraction in surface water bodies. This index has the capability to generate water maps from different satellite images with various resolutions, as many sensors provide images in the green and NIR bands, such as Sentinel-2, MODIS, and China-Brazil Earth-Resources Satellite (CBERS), among others. The results indicate that NGWI performs better than commonly used indices like NDWI, MNDWI, and AWEI. In particular, NGWI can better identify artificial water structures and riparian zones. This improved performance can be attributed to the specific adjustment of convergence coefficient thresholds of the green and NIR bands, as well as the proper use of the newly processed spectral bands from Landsat-9, and significant reductions in incorrect classifications due to shadows and solar glare (USGS, 2023). However, aquatic areas that mix with algae, suspended solids, or macrophytes still present significant confusion for all indices, including NGWI. Although the study focused on the semi-arid region, NGWI showed significant performance for mapping and monitoring water bodies, with the potential for application across the entire national territory.

Overall, NGWI and WRI offered satisfactory results as they effectively suppress other objects in the

image, although an instability in the distribution of pixel values in water masses was observed for NGWI. This pattern may be associated with the sensitivity of the near infrared (NIR) and green bands, which present significant reflectance due to the photosynthetic activity of algae. It is worth mentioning that the Itaparica reservoir exhibits high psychoculture and agricultural activity in its vicinity, factors that can influence the biological and physical characteristics of the water. On the other hand, this behavior was mitigated in the WRI index due to the inclusion of the shortwave infrared (SWIR) band in its formulation. The high absorption of this band in water bodies results in a stabilization of pixel values in the water, contributing to overcoming the instability observed in NGWI, which resulted in better detection estimates. The results found for the WRI agreed with the findings of Herndon et al. (2020), Laonamsa et al. (2023) and especially Deoli et al. (2021), who evaluated the quality of mapping of various lakes in India using Landsat images, GPS lake physical survey and NDWI, MNDWI, WRI, NDVI indices and found that high performance was achieved by WRI comparing with other indices.

Finally, according to Zhou et al. (2017) different types of water bodies exhibit distinct reflectance patterns. For example, in water bodies with high concentrations of phytoplankton, reflectance peaks are observed in the green band, while those with high sediment concentrations, such as silt, show reflectance peaks in the red band. Because each water index has a specific combination of spectral bands, its performance in extracting a particular type of water body is optimized or limited. Therefore, it would not be efficient to rely exclusively on a single water index to extract water bodies in a large region, where different types are interspersed. Achieving greater accuracy in mapping large-scale water bodies can be achieved using a combination of different water indices.

All indices analyzed had satisfactory performance in separating water pixels from other pixels, on the other hand, the following stands out: (1) WRI separates water pixels with greater visibility. (2) The NGWI showed the largest median disparity between “Water” pixels and “No-Water” pixels followed by the AWEI index and the WRI. (3) The AWEI and NDWI indices presented the highest mean separability values, although close. (4) The NDWI and MNDWI indices showed significant average correlations of lower yield between the “Water” pixels and the “Non-Water” pixels driven by the proximity of values found for the tree and shrub vegetation classes. The study suggests that water indices are beneficial for the extraction of water bodies which will help researchers in quickly assessing water bodies in the semi-arid region. The various water spectral indices may differ in their behavior and application as found in this study, therefore, the user must also evaluate the conditions of use and soil coverage in the environment, the available bands and the respective specific purpose. Finally, the NGWI is proposed as an alternative and improved water index, capable of effectively extracting large water bodies and extensive river channels. It is particularly useful for extracting water information in semi-arid regions, where moderately noisy results are expected due to the presence of macrophytes and suspended solids. This new method would also be suitable for studies detecting changes in surface waters, as it classifies edge pixels and significantly highlights water bodies in the images. However, a detailed threshold analysis was not tested in this study.

Authors' Contributions

The author was responsible for research, conceptualization, writing, review and final editing.

Interest conflicts

There is no conflict of interest.

References

ALBERTINI, C.; IACOBELLIS, V.; MANFREDA, S. Detection of Surface Water and Floods with Multispectral Satellites. **Remote Sensing**, [S.L.], v. 14, n. 23, p. 6005, 27 nov. 2022. MDPI AG. http://dx.doi.org/10.3390/rs14236005.

ALI, M. I.; DIRAWAN, G. D.; HASIM, A. H.; ABIDIN, M. R. Detection of Changes in Surface Water Bodies

Urban Area with NDWI and MNDWI Methods. **International Journal On Advanced Science, Engineering And Information Technology**, [S.L.], v. 9, n. 3, p. 946, 30 jun. 2019. Insight Society. http://dx.doi.org/10.18517/ijaseit.9.3.8692.

ARST, K. Í. Optical properties and remote sensing of multicomponental water bodies. **Springer Science & Business Media**, 2003.

BARBOSA, C. C. F; NOVO, M. E. M. L.; MARTINS, V. S. (Ed.). **Introdução ao sensoriamento remoto de sistemas aquáticos: princípios e aplicações**. Instituto Nacional de Pesquisas Espaciais, 2019.

BHAGA, T. D.; DUBE, T.; SHEKEDE, M. D.; SHOKO, C. Impacts of Climate Variability and Drought on Surface Water Resources in Sub-Saharan Africa Using Remote Sensing: a review. **Remote Sensing**, [S.L.], v. 12, n. 24, p. 4184, 21 dez. 2020. MDPI AG. http://dx.doi.org/10.3390/rs12244184.

BIJEESH, T. V.; NARASIMHAMURTHY, K. N. Surface water detection and delineation using remote sensing images: a review of methods and algorithms. **Sustainable Water Resources Management**, [S.L.], v. 6, n. 4, p. 100-120, 9 jul. 2020. Springer Science and Business Media LLC. http://dx.doi.org/10.1007/s40899-020-00425-4.

BLACKMORE, D. S. "**Use of Water Indices Derived from Landsat OLI Imagery and GIS to Estimate the Hydrologic Connectivity of Wetlands in the Tualatin River National Wildlife Refuge**." Thesis, Portland State University, 2016. http://pqdtopen.proquest.com/#viewpdf?dispub=10191067.

BROWN, C. F.; BRUMBY, S. P.; GUZDER-WILLIAMS, B.; BIRCH, T.; HYDE, S. B.; MAZZARIELLO, J.; CZERWINSKI, W.; PASQUARELLA, V. J.; HAERTEL, R.; ILYUSHCHENKO, S.. Dynamic World, Near real-time global 10 m land use land cover mapping. **Scientific Data**, [S.L.], v. 9, n. 1, p. 251, 9 jun. 2022. Springer Science and Business Media LLC. http://dx.doi.org/10.1038/s41597-022-01307-4.

CHEN, F.; CHEN, X.; VOORDE, T. V.; ROBERTS, D.; JIANG, H.; XU, W. Open water detection in urban environments using high spatial resolution remote sensing imagery. **Remote Sensing of Environment**, [S.L.], v. 242, p. 111706, jun. 2020. Elsevier BV. http://dx.doi.org/10.1016/j.rse.2020.111706

CHOUDHARY, S. S.; GHOSH, S. K. Surface Water Area Extraction by Using Water Indices and DFPS Method Applied to Satellites Data. **Sensing and Imaging**, [S.L.], v. 23, n. 1, p. 100-120, 26 out. 2022. Springer Science and Business Media LLC. http://dx.doi.org/10.1007/s11220-022-00403-4

CHUVIECO, E.; MARTÍN, M. P.; PALACIOS, A. Assessment of different spectral indices in the red-near-infrared spectral domain for burned land discrimination. **International Journal of Remote Sensing**, [S.L.], v. 23, n. 23, p. 5103-5110, jan. 2002. Informa UK Limited. http://dx.doi.org/10.1080/01431160210153129.

CORDEIRO, M. C. R.; MARTINEZ, J. M.; PEÑA-LUQUE, S. Automatic water detection from multidimensional hierarchical clustering for Sentinel-2 images and a comparison with Level 2A processors. **Remote Sensing of Environment**, [S.L.], v. 253, p. 112209, fev. 2021. Elsevier BV. http://dx.doi.org/10.1016/j.rse.2020.112209.

DEOLI, V.; KUMAR, D.; KUMAR, M.; KURIQI, A.; ELBELTAGI, A. Water spread mapping of multiple lakes using remote sensing and satellite data. **Arabian Journal of Geosciences**, [S.L.], v. 14, n. 21, p. 100-120, 27 out. 2021. Springer Science and Business Media LLC. http://dx.doi.org/10.1007/s12517-021-08597-9

ELSAYED, S.; GAD, M.; FAROUK, M.; SALEH, A. H.; HUSSEIN, H.; ELMETWALLI, A. H.; ELSHERBINY, O.; MOGHANM, F. S.; MOUSTAPHA, M. E.; TAHER, M. A. Using Optimized Two and Three-Band Spectral Indices and Multivariate Models to Assess Some Water Quality Indicators of Qaroun Lake in Egypt. **Sustainability**, [S.L.], v. 13, n. 18, p. 10408, 18 set. 2021. MDPI AG. http://dx.doi.org/10.3390/su131810408.

FEYISA, G. L.; MEILBY, H.; FENSHOLT, R.; PROUD, S. R. Automated Water Extraction Index: a new technique for surface water mapping using landsat imagery. **Remote Sensing Of Environment**, [S.L.], v. 140, p. 23-35, jan. 2014. Elsevier BV. http://dx.doi.org/10.1016/j.rse.2013.08.029

HERNDON, K.; MUENCH, R.; CHERRINGTON, E.; GRIFFIN, R. An Assessment of Surface Water

Detection Methods for Water Resource Management in the Nigerien Sahel. **Sensors**, [S.L.], v. 20, n. 2, p. 431, 12 jan. 2020. MDPI AG. http://dx.doi.org/10.3390/s20020431.

KHAN, R. H. N. Study of Fluctuations in Surface Area of Lake Haramaya using NDWI and MNDWI Methods. **Jgise: Journal of Geospatial Information Science and Engineering**, [S.L.], v. 5, n. 1, p. 36, 30 jun. 2022. Universitas Gadjah Mada. http://dx.doi.org/10.22146/jgise.68630

KAUFMAN, Y.J.; REMER, L.A.. Detection of forests using mid-IR reflectance: an application for aerosol studies. **Ieee Transactions On Geoscience And Remote Sensing**, [S.L.], v. 32, n. 3, p. 672-683, maio 1994. Institute of Electrical and Electronics Engineers (IEEE). http://dx.doi.org/10.1109/36.297984

KUTSER, T.; HEDLEY, J.; GIARDINO, C.; ROELFSEMA, C.; BRANDO, V. E. Remote sensing of shallow waters – A 50 year retrospective and future directions. Remote Sensing of Environment, [S.L.], v. 240, p. 111619, abr. 2020. Elsevier BV. http://dx.doi.org/10.1016/j.rse.2019.111619.

LAONAMSAI, J.; JULPHUNTHONG, P.; SAPRATHET, T.; KIMMANY, B.; GANCHANASURAGIT, T.; CHOMCHEAWCHAN, P.; TOMUN, N. Utilizing NDWI, MNDWI, SAVI, WRI, and AWEI for Estimating Erosion and Deposition in Ping River in Thailand. **Hydrology**, [S.L.], v. 10, n. 3, p. 70, 19 mar. 2023. MDPI AG. http://dx.doi.org/10.3390/hydrology10030070

LEE, Z.; CARDER, K.; ARNONE, R.; HE, M.. Determination of Primary Spectral Bands for Remote Sensing of Aquatic Environments. **Sensors**, [S.L.], v. 7, n. 12, p. 3428-3441, 20 dez. 2007. MDPI AG. http://dx.doi.org/10.3390/s7123428.

LI, M.; WU, P.; WANG, B.; PARK, H.; HUI, Y.; YANLAN, W. A Deep Learning Method of Water Body Extraction From High Resolution Remote Sensing Images With Multisensors. **Ieee Journal Of Selected Topics In Applied Earth Observations And Remote Sensing**, [S.L.], v. 14, p. 3120-3132, 2021. Institute of Electrical and Electronics Engineers (IEEE). http://dx.doi.org/10.1109/jstars.2021.3060769

MA, S.; ZHOU, Y.; GOWDA, P. H.; DONG, J.; ZHANG, G.; KAKANI, V. G.; WAGLE, P.; CHEN, L.; FLYNN, K. C.; JIANG, W. Application of the water-related spectral reflectance indices: a review. **Ecological Indicators**, [S.L.], v. 98, p. 68-79, mar. 2019. Elsevier BV. http://dx.doi.org/10.1016/j.ecolind.2018.10.049.

MARTÍN, M. P.; GÓMEZ, I.; CHUVIECO, E. Burnt Area Index (BAIM) for burned area discrimination at regional scale using MODIS data. **Forest Ecology and Management**, [S.L.], v. 234, p. 221, nov. 2006. Elsevier BV. http://dx.doi.org/10.1016/j.foreco.2006.08.248.

MCFEETERS, S. K. The use of the Normalized Difference Water Index (NDWI) in the delineation of open water features. **International Journal of Remote Sensing**, [S.L.], v. 17, n. 7, p. 1425-1432, maio 1996. Informa UK Limited. http://dx.doi.org/10.1080/01431169608948714.

MOSTAFA, Y. A Review on Various Shadow Detection and Compensation Techniques in Remote Sensing Images. **Canadian Journal of Remote Sensing**, [S.L.], v. 43, n. 6, p. 545-562, 18 out. 2017. Informa UK Limited. http://dx.doi.org/10.1080/07038992.2017.1384310.

MUSIE, W.; GONFA, G. Fresh water resource, scarcity, water salinity challenges and possible remedies: a review. **Heliyon**, [S.L.], v. 9, n. 8, p. 1-18, ago. 2023. Elsevier BV. http://dx.doi.org/10.1016/j.heliyon.2023.e18685

PURNAM, K. K.; PRASAD, A. D.; GANASALA, P. Water indices for surface water extraction using geospatial techniques: a brief review. **Sustainable Water Resources Management**, [S.L.], v. 10, n. 2, p. 100-120, 5 mar. 2024. Springer Science and Business Media LLC. http://dx.doi.org/10.1007/s40899-024-01035-0

OUMA, Y. O.; TATEISHI, R. A water index for rapid mapping of shoreline changes of five East African Rift Valley lakes: an empirical analysis using Landsat TM and ETM+ data. **International Journal of Remote Sensing**, [S.L.], v. 27, n. 15, p. 3153-3181, 10 ago. 2006. Informa UK Limited. http://dx.doi.org/10.1080/01431160500309934.

OTSU, N. A Threshold Selection Method from Gray-Level Histograms. Ieee Transactions On Systems, Man, And Cybernetics, [S.L.], v. 9, n. 1, p. 62-66, jan. 1979. **Institute of Electrical and Electronics Engineers**

(IEEE). http://dx.doi.org/10.1109/tsmc.1979.4310076

SABALE, R.; VENKATESH, B.; JOSE, Mathew. Sustainable water resource management through conjunctive use of groundwater and surface water: a review. **Innovative Infrastructure Solutions**, [S.L.], v. 8, n. 1, p. 42-72, 11 nov. 2022. Springer Science and Business Media LLC. http://dx.doi.org/10.1007/s41062-022-00992-9

TANG, W.; ZHAO, C.; LIN, J.; JIAO, C.; ZHENG, G.; ZHU, J.; PAN, X.; HAN, X. Improved Spectral Water Index Combined with Otsu Algorithm to Extract Muddy Coastline Data. **Water**, [S.L.], v. 14, n. 6, p. 855, 9 mar. 2022. MDPI AG. http://dx.doi.org/10.3390/w14060855

TENG, J.; XIA, S.; LIU, Y.; YU, X.; DUAN, H.; XIAO, H.; ZHAO, C. Assessing habitat suitability for wintering geese by using Normalized Difference Water Index (NDWI) in a large floodplain wetland, China. **Ecological Indicators**, [S.L.], v. 122, p. 107260, mar. 2021. Elsevier BV. http://dx.doi.org/10.1016/j.ecolind.2020.107260

SAGAN, V.; PETERSON, K. T.; MAIMAITIJIANG, M.; SIDIKE, P.; SLOAN, J.; GREELING, B. A.; MAALOUF, S.; ADAMS, C. Monitoring inland water quality using remote sensing: potential and limitations of spectral indices, bio-optical simulations, machine learning, and cloud computing. **Earth-Science Reviews**, [S.L.], v. 205, p. 103187, jun. 2020. Elsevier BV. http://dx.doi.org/10.1016/j.earscirev.2020.103187.

SOLTANIAN, F. K.; ABBASI, M.; BAKHTYARI, H. R. R. Flood Monitoring Using NDWI And MNDWI Spectral Indices: a case study of aghqala flood-2019, golestan province, Iran. **The International Archives of The Photogrammetry, Remote Sensing and Spatial Information Sciences**, [S.L.], v. -4/18, p. 605-607, 18 out. 2019. Copernicus GmbH. http://dx.doi.org/10.5194/isprs-archives-xlii-4-w18-605-2019.

SHEN, L.; LI, C. **Water body extraction from Landsat ETM+ imagery using adaboost algorithm**. 2010 18Th International Conference On Geoinformatics, [S.L.], p. 100-120, jun. 2010. IEEE. http://dx.doi.org/10.1109/geoinformatics.2010.5567762.

RAD, A. M.; KREITLER, J.; SADEGH, M. Augmented Normalized Difference Water Index for improved surface water monitoring. **Environmental Modelling & Software**, [S.L.], v. 140, p. 105030, jun. 2021. Elsevier BV. http://dx.doi.org/10.1016/j.envsoft.2021.105030

RAWAT, K. S.; SAHU, S. R.; SINGH, S. K.; CHANDER, S.; GUJRATI, A. Water Quality Analysis Using Normalized Difference Chlorophyll Index (NDCI) and Normalized Difference Turbidity Index (NDTI), Using Google Earth Engine Platform. **International Conference On Modeling, Simulation &Amp; Intelligent Computing (Mosicom)**, [S.L.], p. 42-72, 7 dez. 2023. IEEE. http://dx.doi.org/10.1109/mosicom59118.2023.10458842.

TEW, Y. L.; TAN, M. L.; SAMAT, N.; CHAN, N. W.; MAHAMUD, M. A.; SABJAN, M. A.; LEE, L. K.; SEE, K. F.; WEE, S. T. Comparison of Three Water Indices for Tropical Aquaculture Ponds Extraction using Google Earth Engine. **Sains Malaysiana**, [S.L.], v. 51, n. 2, p. 369-378, 28 fev. 2022. Penerbit Universiti Kebangsaan Malaysia (UKM Press). http://dx.doi.org/10.17576/jsm-2022-5102-04.

USGS, U. S. G. S. **"Landsat 8-9 Collection 2 Level 2 Science Product Guide | U.S. Geological Survey**.". 2023, www.usgs.gov/media/files/landsat-8-9-collection-2-level-2-science-product-guide

VERMOTE, E.; JUSTICE, C.; CLAVERIE, M.; FRANCH, B. Preliminary analysis of the performance of the Landsat 8/OLI land surface reflectance product. **Remote Sensing of Environment**, [S.L.], v. 185, p. 46-56, nov. 2016. Elsevier BV. http://dx.doi.org/10.1016/j.rse.2016.04.008

ZHOU, Y; DONG, J.; XIAO, X.; XIAO, T.; YANG, Z.; ZHAO, G.; ZOU, Z.; QIN, Y. Open Surface Water Mapping Algorithms: a comparison of water-related spectral indices and sensors. **Water**, [S.L.], v. 9, n. 4, p. 256, 5 abr. 2017. MDPI AG. http://dx.doi.org/10.3390/w9040256

WALT, S. V. D.; SCHÖNBERGER, J. L.; NUNEZ-IGLESIAS, J.; BOULOGNE, F.; WARNER, J. D.; YAGER, N.; GOUILLART, E.; YU, T. Scikit-image: image processing in python. Peerj, [S.L.], v. 2, p. 453, 19 jun. 2014. **PeerJ**. http://dx.doi.org/10.7717/peerj.453.

WANG, Z.; LIU, J.; LI, J.; ZHANG, D. Multi-Spectral Water Index (MuWI): a native 10-m multi-spectral

water index for accurate water mapping on sentinel-2. **Remote Sensing**, [S.L.], v. 10, n. 10, p. 1643, 16 out. 2018. MDPI AG. http://dx.doi.org/10.3390/rs10101643

WEN, Zhaofei; ZHANG, Ce; SHAO, Guofan; WU, Shengjun; ATKINSON, Peter M.. Ensembles of multiple spectral water indices for improving surface water classification. **International Journal Of Applied Earth Observation And Geoinformation**, [S.L.], v. 96, p. 102278, abr. 2021. Elsevier BV. http://dx.doi.org/10.1016/j.jag.2020.102278

WICAKSONO, A.; WICAKSONO, P. Geometric Accuracy Assessment for Shoreline Derived from NDWI, MNDWI, and AWEI Transformation on Various Coastal Physical Typology in Jepara Regency using Landsat 8 OLI Imagery in 2018. **Geoplanning: Journal of Geomatics and Planning**, [S.L.], v. 6, n. 1, p. 55, 30 ago. 2019. Institute of Research and Community Services Diponegoro University (LPPM UNDIP). http://dx.doi.org/10.14710/geoplanning.6.1.55-72

XIE, H.; LUO, X.; XU, X.; PAN, H.; TONG, X. Evaluation of Landsat 8 OLI imagery for unsupervised inland water extraction. **International Journal of Remote Sensing**, [S.L.], v. 37, n. 8, p. 1826-1844, 11 abr. 2016. Informa UK Limited. http://dx.doi.org/10.1080/01431161.2016.1168948.

XU, H. Modification of normalised difference water index (NDWI) to enhance open water features in remotely sensed imagery. **International Journal of Remote Sensing**, [S.L.], v. 27, n. 14, p. 3025-3033, 20 jul. 2006. Informa UK Limited. http://dx.doi.org/10.1080/01431160600589179.

YUE, H.; LI, Y.; QIAN, J.; LIU, Y. A new accuracy evaluation method for water body extraction. **International Journal of Remote Sensing**, [S.L.], v. 41, n. 19, p. 7311-7342, 7 jul. 2020. Informa UK Limited. http://dx.doi.org/10.1080/01431161.2020.1755740

YANG, J.; DU, X. An enhanced water index in extracting water bodies from Landsat TM imagery. **Annals Of Gis**, [S.L.], v. 23, n. 3, p. 141-148, 16 jun. 2017. Informa UK Limited. http://dx.doi.org/10.1080/19475683.2017.1340339.

Main Author Biography

Juarez Antônio da Silva Júnior was born in Recife, PE – Brazil. He has a degree in Cartographic Engineering and Surveying from the Federal University of Pernambuco-UFPE (2021) and is currently a master's student in the Postgraduate Program in Civil Engineering (PPGEC) with an emphasis on Remote Sensing applied to Water Resources.